Journal of Molecular Catalysis A: Chemical 318 (2010) 36–43

Contents lists available at ScienceDirect

Journal of Molecular Catalysis A: Chemical

journal homepage: www.elsevier.com/locate/molcata

Partial oxidation of methanol over copper catalysts supported on rice husk ash

Wun-Syong Chen, Feg-Wen Chang*, L. Selva Roselin, Ti-Cheng Ou, Szu-Chia Lai

Department of Chemical and Materials Engineering, National Central University, 300 Jungda Rd., Chungli 32001, Taiwan

ARTICLE INFO

Article history:
Received 30 July 2009
Received in revised form 3 November 2009
Accepted 4 November 2009
Available online 10 November 2009

Keywords:
Copper catalyst
Rice husk ash support
Methanol partial oxidation
Hydrogen
Deposition–precipitation

ABSTRACT

Copper catalysts supported on rice husk ash (Cu/RHA) were tested for partial oxidation of methanol (POM) to produce H_2. The catalysts were prepared by deposition–precipitation and characterized by ICP-AES, TGA, XRD, TPR, XPS and N_2O titration techniques. The Cu/RHA catalyst with 10.2 wt.% Cu loading and under 673 K calcination has higher copper dispersion and smaller Cu particle size. This catalyst exhibits higher activity and selectivity for POM to produce H_2. The partial pressure of O_2 plays an important role to determine the product distribution. Catalytic activity of the catalyst at different reaction temperatures shows that CH_3OH conversion, H_2 selectivity and CO selectivity increase with rise in temperature. At different temperatures along with POM, several reactions such as methanol combustion, steam reforming of methanol, methanol decomposition, water gas shift and oxidation of CO and H_2 might be involved. Comparison of catalytic activity of Cu/RHA and Cu/SiO_2 catalysts demonstrates that Cu/SiO_2 catalysts deactivate with time with faster rate and have higher CO selectivity. This proves that Cu/RHA catalysts have good thermal stability and selectivity for POM to produce H_2.

1. Introduction

Polymer electrolyte fuel cells (PEMFCs) using H_2 fuels have been attractive because of their high power density, low operation temperature, low emissions of NO_x, greenhouse gas and so on [1]. It has been applied to various fields such as transportation, stationary and portable applications [2–6]. Methanol is an excellent hydrogen carrier because of its high energy density, easy availability, safe storage etc. It produces less CO and can be activated at relatively low temperature compared to other fuels, such as natural gas, ethanol and gasoline [7]. There are several reaction pathways for methanol to produce hydrogen, such as methanol decomposition (MD, Eq. (1)) [8], steam reforming of methanol (SRM, Eq. (2)) [9,10], oxidative steam reforming of methanol (OSRM, Eq. (3)) [11,12] and partial oxidation of methanol (POM, Eq. (4)) [13,14]:

$$CH_3OH \rightarrow 2H_2 + CO \quad (1)$$

$$CH_3OH + H_2O \rightarrow 3H_2 + CO_2 \quad (2)$$

$$CH_3OH + 0.5H_2O + 0.25O_2 \rightarrow 2.5H_2 + CO_2 \quad (3)$$

$$CH_3OH + 0.5O_2 \rightarrow 2H_2 + CO_2 \quad (4)$$

Methanol decomposition (MD) produces CO and the presence of CO in the gas fed to fuel cell stack will deteriorate the anode catalyst and lower the system efficiency of PEMFC [15]. Partial oxidation of methanol (POM) exhibits some advantages over the other reactions. It uses air or oxygen instead of steam and so no need to equip with steam generation unit. Also it is an exothermic reaction and has higher reaction rate and so it can shorten the reaction time to reach the working temperature from start-up conditions. POM has been investigated over supported Pd, Pt, Au catalysts [16–20]. In addition, Cu-based catalysts have been the most generally studied catalysts [21,22] but there are not many researches over silica-supported Cu catalysts.

Rice husk is the milling by-product of rice and is the major waste product of agriculture industry. It is usually burned or discarded, causing serious environmental pollutions. Therefore, utilization of the rice husk for useful purpose is necessary. In our previous study we found that these rice husks can be used as a support after converting them into silica [23,24]. A series of processes such as acid leaching, pyrolysis and carbon removing lead to the formation of 99% pure amorphous rice husk ash (RHA). It exhibited high activity when these were used as a catalyst support materials. For example, RHA-supported Ni and Cu catalysts have shown good activity for CO_2 hydrogenation and ethanol dehydrogenation, respectively [23,24].

Adam research group have reported various metal ions incorporated RHA catalysts for Friedel–Craft benzylation and oxidation reactions [25–30]. For instance, Fe-RHA for Friedel–Craft benzylation of toluene; Al, Ga, Fe and In-incorporated RHA catalysts for the Friedel–Craft benzylation of benzene and substituted benzenes; Ga, In and Fe-incorporated RHA catalysts for Friedel–Craft benzylation of p-xylene. Chromium and 4-(methylamino)benzoic acid (MBA) incorporated RHA catalysts were reported to be active for the oxi-

* Corresponding author. Tel.: +886 3 4227151x34202; fax: +886 3 4252296.
E-mail address: fwchang@cc.ncu.edu.tw (F.-W. Chang).

1381-1169/$ – see front matter © 2009 Elsevier B.V. All rights reserved.
doi:10.1016/j.molcata.2009.11.005

dation of cyclohexane under mild reaction conditions. It was shown that these catalysts could be reused successively for several times.

In the present study, we have investigated RHA-supported Cu catalysts for partial oxidation of methanol (POM) to produce hydrogen. To obtain an efficient catalytic system, the reaction parameters such as copper loading, calcination temperature, O_2/CH_3OH molar ratio and reaction temperature were optimized. In addition, under the optimum conditions the activity of this catalyst (Cu/RHA) was compared with copper supported on commercial silica gel (Cu/SiO_2). Several techniques were employed to identify the characteristics of the catalyst, such as inductively coupled plasma atomic emission spectroscopy (ICP-AES), thermal gravimetric analysis (TGA), X-ray diffraction (XRD), X-ray photoelectron spectroscopy (XPS), temperature-programmed reduction (TPR) analysis and N_2O titration.

2. Experimental

2.1. Pre-treatment of raw material

The raw material, rice husk, was obtained from a rice mill. The rice husk was washed thoroughly with reverse osmosis water in order to remove adhering soil and then it was dried in an air oven at 373 K for 24 h. The processes of acid leaching, pyrolysis, and carbon removing were carried out as reported in our previous work [23,24,31–33]. The dried rice husk was refluxed with 3 N HCl at its boiling point in a glass round-bottomed flask for 1 h. It was then filtered and washed thoroughly with warm deionized water until the filtrate was free from acid. The leached rice husk was then dried at 373 K for 24 h. The pyrolysis was carried out in the atmosphere of nitrogen at 1173 K for 1 h by placing the treated rice husk in a quartz tubular reactor. After pyrolysis, the rice husk was heated in an air furnace at 1173 K for 1 h to remove carbon. The white rice husk ash was obtained with amorphous silica content higher than 99%. It was used as a support material for catalyst preparation and designated as RHA.

2.2. Catalyst preparation

The copper catalysts supported on RHA were prepared by the deposition–precipitation technique using the hydrolysis of urea at 363 K to raise the pH. The main procedures were referred to van der Grift et al. [34]. First, the copper solution was prepared by dissolving urea (Merck) and copper nitrate pentahemihydrate ($Cu(NO_3)_2{\cdot}2.5H_2O$, Riedel-deHaën), according to the given catalyst composition; per equivalent copper, three equivalents urea was used. Then a required amount of RHA was suspended. The suspension was heated to 363 K and the pH was adjusted to 2–3 by the addition of nitric acid for 2 h. The solution was continuously stirred for 14 h at 363 K. After complete precipitation, the suspension was filtered and the sample was washed with hot deionized water (363 K). These samples were dried in an air oven at 373 K for 24 h and denoted as Cu/RHA catalyst precursors, which were subsequently calcined in an air furnace at different temperatures for 4 h. Finally, the calcined samples were reduced at 573 K for 1 h to give the final catalysts, which were denoted as Cu/RHA catalysts. The same preparation procedure was adopted for preparing copper catalyst supported on commercial silica gel (Merck), which was denoted as Cu/SiO_2 catalysts. Unsupported copper oxide was prepared by calcination of copper nitrate pentahemihydrate at 673 K for 4 h.

2.3. Catalyst characterization

The metallic impurities of supports and copper content of Cu/RHA catalysts were determined by inductively coupled plasma atomic emission spectrometer (ICP-AES, Jobin Yvon JY-38S). Prior to analysis, the catalysts were dissolved in aqua regia (HNO_3:HCl, in 1:3 ratio) and diluted within the detection limit of the instrument.

TGA measurements were carried out in air with the aid of PerkinElmer TGA-7. The sample was dried at 373 K and then heated from 373 to 1173 K at a heating rate of 10 K/min.

X-ray diffraction (XRD) was used to identify the copper species on the catalysts. X-day diffractometer (Bruker, D8A) was operated at 40 kV and 30 mA using Cu Kα radiation with a wavelength of 1.5406 Å. The scanning angle has been set (Bragg angle 2θ) from 10° to 80° at a rate of 0.02°/s.

Temperature-programmed reduction (TPR) was performed in a U-shaped micro-reactor made of quartz, surrounded with a furnace controlled by a programmed heating system. Prior to the experiment, 80 mg of the catalyst sample was dried under flowing Ar (50 ml/min) at room temperature for 45 min. A reducing gas composed of 5% H_2 plus 95% Ar was employed at a flow rate of 50 ml/min, with a heating ramp of 10 K/min from 323 to 873 K. The hydrogen consumption was determined by gas chromatography equipped with a thermal conductivity detector (TCD).

The chemical states of copper in Cu/RHA catalysts after different pre-treatments were studied by X-ray photoelectron spectroscopy (XPS). A Thermo VG Scientific Sigma Probe spectrometer equipped with a hemispherical electron analyzer and an Al Kα X-ray radiation source ($h\nu$ = 1486.6 eV) powered at 15 kV and 7.2 mA was used for the analysis. The residual pressure in the analyst's chamber was below 5×10^{-9} Torr. The binding energies (BE) were determined utilizing C 1s spectra as reference with an energy of 285 eV.

To determine the copper surface area, dispersion and average particle size of the catalysts, N_2O titration was employed. The main procedures were referred to van der Grift et al. [35], who studied the effect of temperature and time for N_2O dissociative chemisorption. Typically, 80 mg of Cu/RHA catalyst after calcination in air at 673 K was first reduced in a reducing gas composed of 5% H_2 plus 95% Ar for 1 h at a flow rate of 50 ml/min, with a heating ramp of 10 K/min from 323 to 573 K. Next, complete bulk oxidation was carried out with O_2 (50 ml/min) at 573 K for 1 h. Second reduction was executed according to the reduction procedure described above. Subsequently the sample was performed with N_2O (50 ml/min) at 363 K for 20 min to surface oxidation. Finally, the sample was reduced again as described above. The reactor was purged with Ar for 10 min before introducing different gases. It was assumed that all the surface copper atoms were oxidized to Cu_2O by N_2O (surface oxidation) and all copper atoms in the catalysts were oxidized to CuO by O_2 (complete bulk oxidation). After surface oxidation, hydrogen consumption provides a measure for the number of surface copper atoms, whereas, hydrogen consumption after complete bulk oxidation provides a measure of total amount of copper in the catalyst.

2.4. Catalytic activity measurements

Prior to start the POM reaction, the calcined samples were reduced with 5% H_2 and 95% Ar gas flow (50 ml/min) at 573 K for 1 h. The reaction was carried out at atmospheric pressure with 80 mg catalyst in a U-shaped quartz micro-reactor (i.d. = 4 mm) which was placed inside a programmable furnace. A K-type thermocouple was used to measure the central temperature of the catalyst bed. The carrier gas Ar and O_2 were controlled by Brooks 5850E mass flow meter with a precision controller (Protec Instrument Co. Ltd. Model: PC-540) to maintain the total flow rate of 40 ml/min. Liquid methanol was fed into an evaporator by means of a peristaltic pump (Cole-Parmer EW-77120-52) at 1.2 ml/h. To optimize the O_2/CH_3OH molar ratio and reaction temperature, the molar ratio of O_2/CH_3OH was varied from 0.1 to 0.6 and the reactor temperature was varied from 473 to 573 K. The reaction products were analyzed

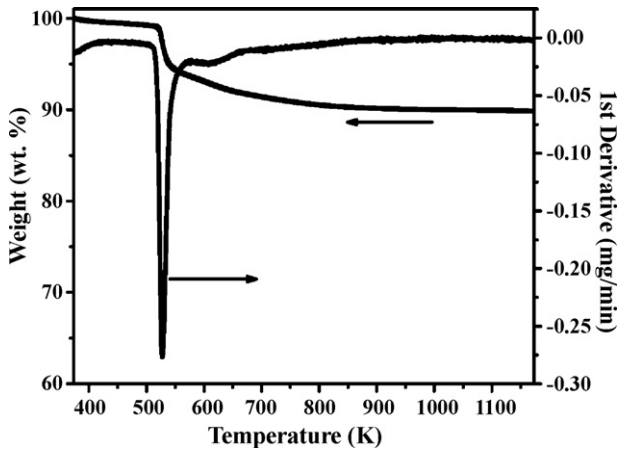

Fig. 1. TGA and DTG curves of 28.9 wt.% Cu/RHA catalyst precursor.

on-line using two gas chromatographs (GC) equipped with thermal conductivity detector and porapak Q and carbosieve S-II columns.

3. Results and discussion

3.1. TGA

In order to understand the chemical changes of the prepared Cu/RHA catalyst precursor during calcination process, thermogravimetric analysis (TGA) was carried out. Fig. 1 illustrates the TGA and DTG curves of 28.9 wt.% Cu/RHA catalyst precursor. The weight loss is ascribed to the decomposition of the copper hydrosilicate structure held on the surface of RHA to form copper oxide. According to van der Grift et al. [34], they prepared silica-supported copper catalyst by the same method and found that highly dispersed copper hydrosilicate were formed and their structural properties were similar to the mineral chrysocolla. In addition, they used in situ diffuse reflectance infrared Fourier-transform (DRIFT) to study the effect of calcination under oxygen atmosphere and suggested that the copper on silica catalysts prepared by deposition–precipitation method decomposed from chrysocolla structure to silica-supported copper oxide [36]. The copper hydrosilicate structure decomposed completely at temperature above 723 K. As seen from Fig. 1, above 673 K there was no further weight loss of 28.9 wt.% Cu/RHA catalyst precursor, which indicates that the hydrosilicate structure was completely decomposed to copper oxide.

3.2. XRD

Fig. 2 presents the XRD patterns of Cu/RHA catalysts with various copper loadings calcined at 673 K along with the pattern of unsupported copper oxide (CuO). CuO, a reference material for analysis was obtained by calcining pure copper nitrate pentahemihydrate. The data was identified precisely to JCPDS file 45-0937 and the results (Fig. 2e) revealed that the copper nitrate pentahemihydrate under thermal treatment had been completely converted to copper oxide. In Fig. 2a–d, a broad peak at $2\theta = 22^{\circ}$ could be associated with amorphous silica presented by the RHA support. This result is similar to the reports of Cu/SiO_2 catalysts [37,38]. These XRD results were similar to other metal incorporated rice husk ash reported earlier [25,29,30]. Yalcin and Sevinc [39] have also reported that the amorphous silica was obtained from rice husk (purity 99.6%). At low copper loadings (5.6 and 10.2 wt.%), no diffraction peak could be detected (Fig. 2a and b). This could be due to the highly dispersed CuO particles, which was too small to be detected by XRD. When the copper loading was 19.2 wt.% and above, two sharp diffraction

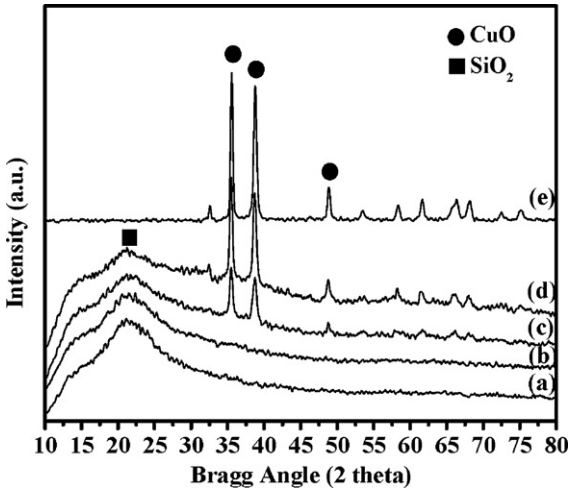

Fig. 2. XRD patterns of: (a) 5.6 wt.%; (b) 10.2 wt.%; (c) 19.2 wt.%; (d) 28.9 wt.% Cu/RHA catalysts and (e) unsupported CuO (all calcined at 673 K for 4 h).

peaks ($2\theta = 35.5$ and 38.7) were appeared (Fig. 2c and d). This was ascribed to a typical structure of the tenorite, a monoclinic structure of CuO with the crystal plane of (1 1 1). Thus, after calcination, the copper species was transformed into CuO, identical to the reference compound. This result agrees with the TGA result, which described that the Cu/RHA catalyst precursor is decomposed from copper hydrosilicate to copper oxide.

3.3. TPR

TPR has been used to characterize the reduction profile of copper metal ions in the supported metal catalysts. The reduction profile provides information about the dispersion of the metal species on the support, metal ion size and interaction between these metal species and the support. TPR was carried out from 323 to 873 K for unsupported CuO, Cu/RHA catalysts with various copper loadings calcined at 673 K and 10.2 wt.% Cu/RHA catalysts calcined at different temperatures. Fig. 3 shows the TPR profiles of unsupported CuO and the Cu/RHA catalysts calcined at 673 K with various copper loadings. The unsupported CuO reduction peak was used to identify bulk CuO on Cu/RHA catalysts. TPR profiles of all examined Cu/RHA catalysts showed a unique narrow reduction peak centered at 492 to 513 K. The unique peak observed can be attributed to a single reduction step: $Cu(II) \rightarrow Cu^0$ suggesting the presence of well dis-

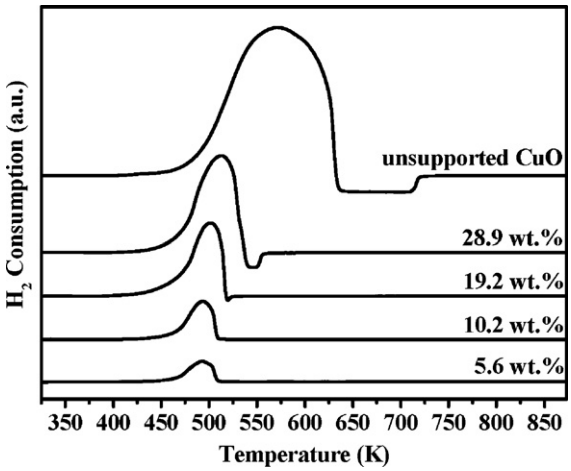

Fig. 3. TPR profiles of unsupported CuO and the Cu/RHA catalysts calcined at 673 K for 4 h with various copper loadings.

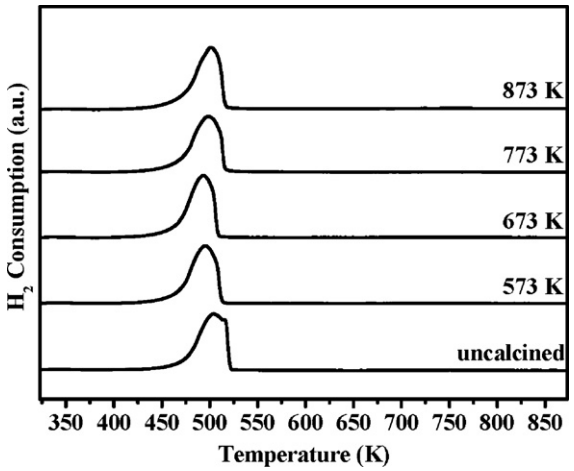

Fig. 4. TPR profiles of 10.2 wt.% Cu/RHA catalysts calcined at different temperatures for 4 h.

persed Cu^{2+} species [40]. The unsupported pure CuO is reduced at considerably higher temperature (570 K). Also, the reduction peak becomes broader, which suggests the heterogeneity of reduction. For the Cu/RHA catalyst system, as expected, the samples with higher copper loading exhibited larger hydrogen consumption. The reduction temperature shifted to higher temperature with increasing copper content. The observed shift may be due to different copper particle sizes, different interactions between copper oxide and silica and different copper oxide dispersions. It was reported that higher temperature is needed for the reduction of larger Cu crystallites [41]. These results are in accordance with XRD results. In addition, the peaks are broadened and become asymmetric at higher copper loading. This may be attributed to the appearance of larger particle sizes, lower dispersions of copper oxide species, and weaker interactions between copper and RHA. The broad reduction peak maybe related to the different size of CuO or the two step reduction: $Cu(II) \rightarrow Cu(I) \rightarrow Cu^0$. According to van der Grift et al. [42], they have observed a hydrogen consumption peak centered at 460 K for Cu/SiO_2 catalyst calcined at 700 K. The reduction temperature for Cu/RHA in the present study is higher than the reported value of van der Grift et al. Even though the T_{max} depends on the heating rate, the hydrogen concentration in the reducing gas, and the operating parameters of the reactor system, the difference might be related to stronger metal–support interaction (MSI) between Cu and RHA [24]. The interaction is stronger, making the reduction process more difficult or slower to occur, resulting in the smaller copper oxide particles or better copper oxide dispersion on the catalyst surface. From the above TPR results at different Cu loadings, it was inferred that there are highly dispersed small CuO on the surface at low copper loading. These highly dispersed CuO are not detectable by XRD. In addition, metal–support interaction (MSI) between Cu and RHA are stronger compared to Cu/SiO_2 catalyst. Fig. 4 shows the TPR profiles of 10.2 wt.% Cu/RHA catalysts calcined at different temperatures for 4 h. The uncalcined sample shows a reduction peak with a shoulder at 515 K. It is due to a discontinuity in the rate of reduction of the chrysocolla-like structure [36]. The relative contribution of two peaks depends on the preparation conditions. Besides, after calcination process, the copper hydrosilicate (chrysocolla) in the precursor was dehydrated and; thereby the color of the catalyst changed from blue (copper ions in chrysocolla were in an octahedral environment) to olive green, characteristic of decomposed chrysocolla with a two dimensional tenorite-on-silica structure. All samples calcined at different temperatures showed single reduction temperature peak, which suggests the homogeneity of CuO species on the surface of the support. But there was a small shift in reduction temperature was observed. This shift may be due to different copper particle sizes in the catalyst. For the sample calcined at 573 and 673 K, the reduction temperature decreased to 495 and 494 K, respectively. This shows that after calcination at lower temperatures, uniform distributions of CuO particles are formed. However, at higher calcination temperature, the reduction temperature is increased to higher temperature. For the sample calcined at 773 and 873 K, the reduction temperature increased to 498 and 501 K, respectively. At higher calcination temperature (773 and 873 K), a few CuO crystallites aggregated leading to the diffusion hindrance by large crystallites. Above results indicate that all copper species are reduced completely below 573 K and so for further catalytic studies all the catalysts were uniformly reduced at 573 K for 1 h.

3.4. Textural properties

Tables 1 and 2 list the surface properties of Cu/RHA catalysts at different copper loadings, 10.2 wt.% Cu/RHA catalysts calcined at different temperatures and 10.3 wt.% Cu/SiO_2 catalysts. When the copper loading increased from 5.6 to 10.2 wt.% in Cu/RHA catalyst, there was only a small decrease in the dispersion of copper was observed; further increase in copper loading resulted in significant decrease in dispersion of copper. In the similar way, but in opposite trend, when the copper loading was increased from 5.6 to 10.2 wt.%, there was no change in the copper crystallite size was observed; but beyond 10.2 wt.% copper loading, significant increase in copper crystallite size was observed. The copper surface area showed a different trend; it reached a maximum when the copper loading was increased to 10.2 wt.% and then diminished while more copper was introduced. These results are in agreement with previous studies on Cu/ZnO catalysts by Alejo et al. [43]. From these results, it was inferred that when adding more copper to the catalyst, larger copper surface area could be attained with high dispersion. But high copper loadings resulted to cause aggregation of copper species leading to larger particle size and lower dispersion. These results are in accordance with TPR and XRD results. Table 2 demonstrates the effect of calcination temperature on the surface properties of 10.2 wt.% Cu/RHA catalyst. The catalyst calcined at 673 K exhibited higher dispersion and smaller Cu particle size compared to uncalcined and those calcined at high temperatures. It was shown that suitable calcination temperature can improve the dispersion of catalyst precursor. However, excessive temperature resulted in sintering of catalyst leading to lower dispersion. It can be deduced that high copper loading and high calcination temperature do not enhance the number of exposed copper species due to the agglomeration of copper clusters as evidenced by the increased size of copper crystallites.

3.5. XPS

In order to understand the chemical state of copper in the Cu/RHA catalyst surface after exposure to different conditions, X-ray photoelectron spectra of Cu/RHA catalysts were collected. Fig. 5 shows the XPS spectra of the Cu $2p_{3/2}$ region for various samples. For dried sample (Fig. 5a), a peak at 935.7 eV and a satellite peak at 942.8 eV were observed. The peak at 935.7 eV was related to $Cu(OH)_2$ component. Since the CuO peak (935.2 eV) is closed to this value, presence of small amount of CuO also could be expected. The satellite peak at 942.8 eV was related to Cu^{2+} ion. After calcination, $Cu(OH)_2$ was completely transformed into CuO, as proved by the peak shift to 935.2 eV (Fig. 5b). This behavior agrees with the TGA and XRD results. Besides, it also indicated that after hydrogen treatment at 573 K for 1 h, reduction of Cu^{2+} and CuO occurred [44]. It could be seen that the CuO peak at 935.2 eV was disappeared completely and a new peak at 932.5 eV was appeared (Fig. 5c).

Table 1
Textural properties of catalysts (Cu/RHA and Cu/SiO_2) calcined at 673 K.

Catalyst	Copper loading (wt.%)[a]	Dispersion (%)[b]	Copper surface area (m^2/g cat.)[b]	Average particle size (nm)[b]
Cu/RHA	5.6	67.8	25.6	1.5
Cu/RHA	10.2	66.4	46.0	1.5
Cu/RHA	19.2	32.8	42.6	3.1
Cu/RHA	28.9	19.3	37.7	5.2
Cu/SiO_2	10.3	58.4	40.7	1.7

[a] ICP-AES method.
[b] N_2O titration method.

Table 2
Textural properties of 10.2 wt.% Cu/RHA catalysts with various calcination temperatures.

Calcination temperature (K)	Dispersion (%)[a]	Copper surface area (m^2/g cat.)[a]	Average particle size (nm)[a]
Uncalcined	46.4	32.1	2.2
573	56.1	38.9	1.8
673	66.4	46.0	1.5
773	58.8	40.7	1.7
873	49.4	34.2	2.0

[a] N_2O titration method.

Since the Cu^0 and Cu^+ exhibited the same binding energy and could not be distinguished from the XPS result. Nevertheless, supporting evidence from TPR analysis shows that the CuO was completely reduced to metallic Cu. In addition the satellite peak at 942.8 for Cu^{2+} was almost disappeared. Alejo et al. [43] have observed the disappearance Cu^{2+} satellite peak and appearance of Cu^0 and Cu^+ peaks upon reduction of Cu/ZnO and $Cu/ZnO/Al_2O_3$ catalysts. In order to analyze the surface property of Cu/RHA catalysts after reaction, the sample after POM reaction at 523 K for 3 h was tested by XPS analysis. The XPS analysis after catalytic test showed an overlapping of 935.2 and 932.5 eV peaks and appearance of a small satellite peak, which indicates that during the POM reaction, the Cu^0 is partially oxidized to CuO under oxygen atmosphere (Fig. 5d). XPS results can be summarized as the catalyst precursor mainly existed as $Cu(OH)_2$. Followed by calcination, the $Cu(OH)_2$ was converted to CuO. The catalyst under reduction treatment, CuO was reduced to Cu^0. In the sample after catalytic test, Cu^0 and CuO were existed.

3.6. Catalytic activity

The catalytic activity and product distribution in the partial oxidation of methanol (POM) over Cu/RHA catalysts were studied. Various parameters such as, copper loading, calcination temperature, O_2/CH_3OH molar ratio and reaction temperature were optimized to produce highly active catalyst for POM to produce hydrogen. It was observed that hydrogen and carbon dioxide were the main products, while water and carbon monoxide were the by-products. No other compounds such as formaldehyde, dimethyl ether, methyl formate or formic acid could be detected, which were observed in other supported copper catalysts. The oxygen conversion throughout all catalytic reaction was closed to 100%. The definitions of methanol conversion, oxygen conversion, hydrogen selectivity and carbon monoxide selectivity are given below:

$$CH_3OH\ \text{conversion}\,(\%) = \left(\frac{\text{moles of } CH_3OH \text{ consumed}}{\text{moles of } CH_3OH \text{ fed}}\right) \times 100$$

$$O_2\ \text{conversion}\,(\%) = \left(\frac{\text{moles of } O_2 \text{ consumed}}{\text{moles of } O_2 \text{ fed}}\right) \times 100$$

$$H_2\ \text{selectivity}\,(\%) = \left(\frac{\text{moles of } H_2 \text{ produced} \times 0.5}{\text{moles of } CH_3OH \text{ consumed}}\right) \times 100$$

$$CO\ \text{selectivity}\,(\%) = \left(\frac{\text{moles of CO produced}}{\text{moles of } CH_3OH \text{ consumed}}\right) \times 100$$

Fig. 6 shows the comparison of catalytic activity of Cu/RHA catalysts with different copper loadings at 523 K with O_2/CH_3OH molar ratio of 0.3. The CH_3OH conversion increased rapidly when copper loading increased from 5.6 to 10.2 wt.%. In excess to 10.2 wt.%

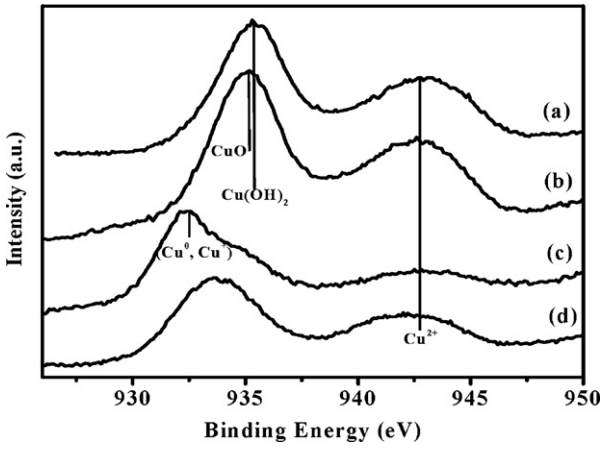

Fig. 5. XPS Cu $2p_{3/2}$ spectra of 10.2 wt.% Cu/RHA catalysts: (a) dried at 373 K; (b) calcined at 673 K for 4 h; (c) reduced at 573 K for 1 h; (d) reacted at 523 K for 3 h.

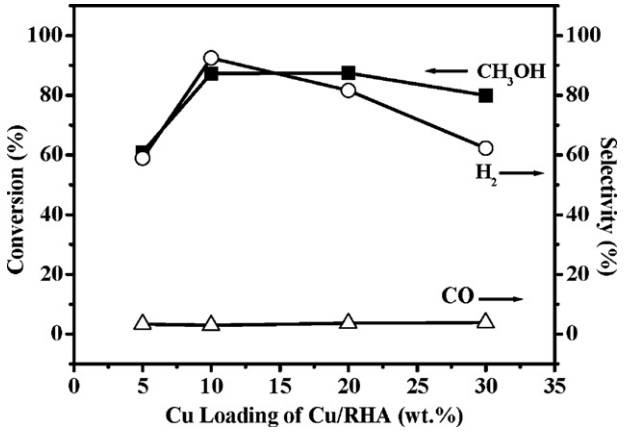

Fig. 6. Effect of copper loading on CH_3OH conversion, H_2 selectivity and CO selectivity for POM over Cu/RHA catalysts (calcination temperature, 673 K; O_2/CH_3OH ratio, 0.3; reaction temperature, 523 K; reaction time, 60 min).

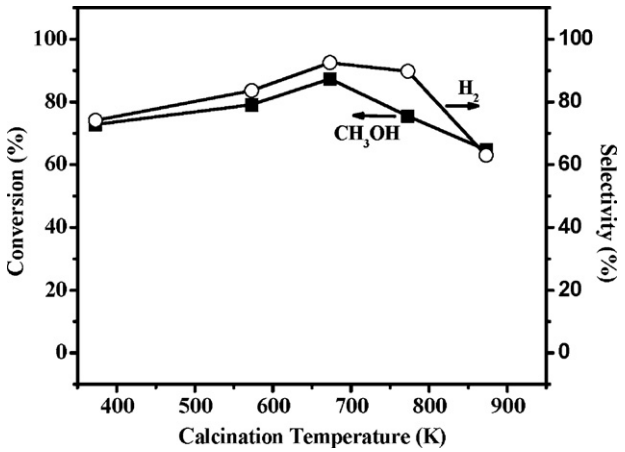

Fig. 7. Effect of calcination temperature on CH_3OH conversion and H_2 selectivity for POM over 10.2 wt.% Cu/RHA catalysts (O_2/CH_3OH ratio, 0.3; reaction temperature, 523 K; reaction time, 60 min).

Cu, there was only a slight increase, followed by an apparent decrease of CH_3OH conversion. The H_2 selectivity reached a maximum at 10.2 wt.% Cu and then dropped when copper loading was higher than 19.2 wt.%. The CO selectivity was similar in all catalysts. The difference in CH_3OH conversion and H_2 selectivity could be explained by analyzing the surface properties of Cu/RHA catalysts at different copper loadings. It was inferred that the Cu/RHA catalyst with 10.2 wt.% exhibited higher copper surface area, smaller copper crystallites and almost higher dispersion. Table 1 shows that the copper surface area reached a maximum when the copper loading was 10.2 wt.%. At higher copper loading, copper surface area decreased with copper loading. It displays the same trend on the H_2 selectivity. Although 5.6 wt.% Cu/RHA catalyst revealed the highest copper dispersion, its low copper surface area lead to lower activity. As seen from figure, the 10.2 wt.% Cu/RHA exhibited the highest catalytic activity and selectivity due to the highest copper surface area and copper dispersion. TPR results also revealed that higher copper loading needed higher reduction temperature, which was due to the increased size of CuO crystallites and the decrease of copper dispersion. It was reported that in supported copper catalysts, the catalysts which showed the highest copper surface area and copper dispersion proved to be an active catalyst for POM to produce hydrogen [44–47]. It was suggested that Cu^0 was active species for selective formation of H_2 by POM [45], whereas Cu^+ favors water and CO formation. Cu^{2+} as CuO exhibited very low activity, producing only water and CO_2. Hence, the 10.2 wt.% Cu/RHA, providing the most Cu^0 exposed on the catalyst surface could enhance the activity for partial oxidation of methanol to produce H_2. For further study 10.2 wt.% Cu/RHA has been used to optimize calcination temperature, O_2/CH_3OH molar ratio and reaction temperature.

The effect of calcination temperature over 10.2 wt.% Cu/RHA catalysts at reaction temperature 523 K with O_2/CH_3OH molar ratio of 0.3 is presented in Fig. 7. It can be seen that the CH_3OH conversion was increased with calcination temperature, reached a maximum at 673 K and then decreased at higher temperature. The H_2 selectivity was also showed the similar trend as that of CH_3OH conversion but the decrease becomes smaller at 773 K. The uncalcined Cu/RHA catalyst exhibited lower activity than those calcined at 673 K. The treatment of calcination results in the highly dispersed copper crystallites and large metallic copper area. Characterization of the catalyst after calcination at different temperatures showed that there was an increase in Cu particle size, decrease in copper dispersion and decrease in copper surface area when the calcination temperature was increased beyond 673 K as evidenced by N_2O titration and TPR analysis. Therefore, the decrease in activity beyond 673 K is due to sintering of active site, which resulted in increase in Cu particle size, decrease in copper dispersion along with decrease in copper surface area. Besides, the influence of calcination temperature on the catalytic activity is smaller between 373 and 773 K. This is due to the strong interaction between copper and silica of the RHA [24]. The strong interaction restricted particles movement and prevented the particles from sintering. This study indicates that the catalyst precursor calcined at 673 K exhibited higher catalytic activity and selectivity towards H_2.

The effect of O_2/CH_3OH molar ratio on the activity of 10.2 wt.% Cu/RHA catalysts, calcined at 673K, was studied at 523K. In Fig. 8, with increasing molar ratio from 0.1 to 0.6, CH_3OH conversion increases from 70.1 to 98.1%. On the other hand, the H_2 selectivity decreases from 99 to 52.1%. According to the work of Fisher and Bell [48], the pre-absorbed oxygen on the catalyst surface was favorable to the chemisorption of methanol and thus the introduction of oxygen was helpful to enhance the activity. However, the decrease in hydrogen selectivity at higher molar ratio could be due to the fast oxidation of H_2 [49,50]. It is important to take into account that the methanol conversion did not tally with the stoichiometry of POM. When the molar ratio was at 0.1 and 0.3, the methanol conversion was higher than the calculated stoichiometry for POM and when the molar ratio was 0.5 and 0.6, the methanol conversion was lower than the calculated stoichiometry for POM. This suggests that other methanol consuming reactions should have participated at lower molar ratio and other oxygen consuming reaction should have participated at higher molar ratio. Theoretically, a molar ratio of 0.1 with complete consumption of oxygen corresponds to 20% conversion of methanol. But experimental result showed that the conversion was higher than 20%. Since all oxygen has consumed, the other methanol consuming reaction that is likely to occur predominantly was methanol decomposition (MD, Eq. (1)) [43,47,50]. This resulted in high CO selectivity and high H_2 selectivity. Nevertheless, the observed CO selectivity was smaller at 0.3 molar ratio. The reason is that CO formed was converted to CO_2 by water gas shift reaction (WGS, Eq. (5)) [47]. For this reaction, water will be utilized and this water was formed by methanol combustion (MC, Eq. (6)).

$$CO + H_2O \rightarrow CO_2 + H_2 \quad (5)$$

$$CH_3OH + 1.5O_2 \rightarrow 2H_2O + CO_2 \quad (6)$$

When the molar ratio was more than the stoichiometry amount required for POM, the contribution of methanol combustion was predominated, which was evidenced by low CO and low H_2 selectiv-

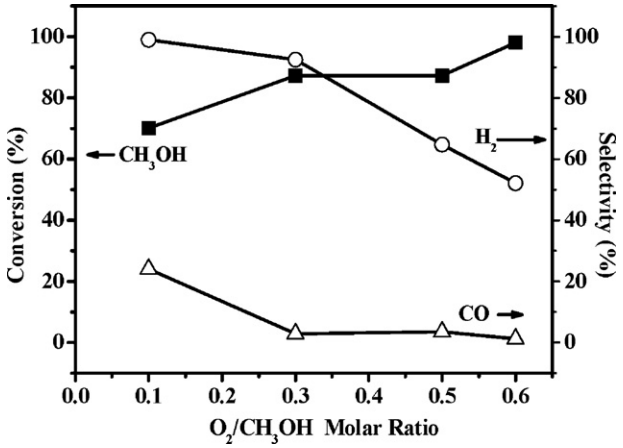

Fig. 8. Effect of O_2/CH_3OH molar ratio on CH_3OH conversion, H_2 selectivity and CO selectivity for POM over 10.2 wt.% Cu/RHA catalysts (calcination temperature, 673 K; reaction temperature, 523 K; reaction time, 60 min).

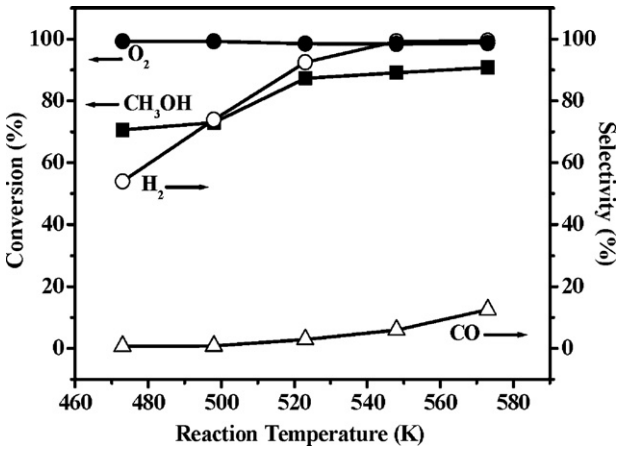

Fig. 9. Effect of reaction temperature on O_2 conversion, CH_3OH conversion, H_2 selectivity and CO selectivity for POM over 10.2 wt.% Cu/RHA catalysts (calcination temperature, 673 K; O_2/CH_3OH ratio, 0.3; reaction time, 60 min).

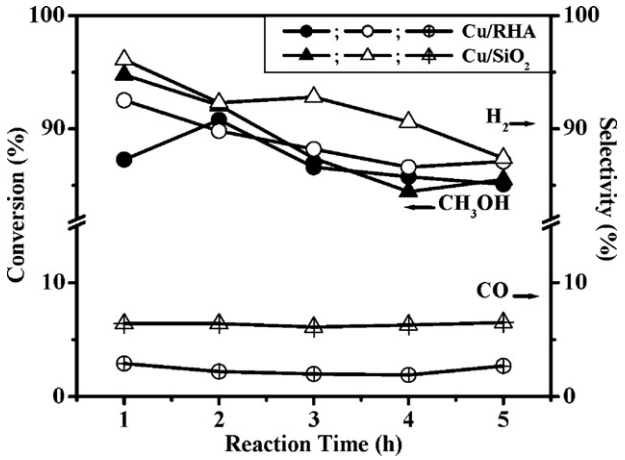

Fig. 10. Comparison of 10.2 wt.% Cu/RHA catalysts and 10.3 wt.% Cu/SiO_2 catalysts on CH_3OH conversion, H_2 selectivity and CO selectivity for POM (calcination temperature, 673 K; O_2/CH_3OH ratio, 0.3; reaction temperature, 523 K).

ity. Likewise, oxidation of H_2 (Eq. (7)) and oxidation of CO (Eq. (8)) reactions may also be favored leading to undesired water formation [17,19].

$$H_2 + 0.5O_2 \rightarrow H_2O \quad (7)$$

$$CO + 0.5O_2 \rightarrow CO_2 \quad (8)$$

Furthermore, at higher molar ratio the catalyst undergo partial or complete oxidation of Cu^0 in the presence of oxygen [44,49]. The oxidized catalyst is inactive for hydrogen production. Therefore, it is apparent that the O_2/CH_3OH molar ratio plays an important role in governing the product distribution. The O_2/CH_3OH molar ratio at 0.3 value exhibited higher CH_3OH conversion and H_2 selectivity.

Fig. 9 shows the effect of reaction temperature on O_2 conversion, CH_3OH conversion, H_2 selectivity and CO selectivity for POM reaction over 10.2 wt.% Cu/RHA catalysts using an O_2/CH_3OH molar ratio of 0.3. The study was undertaken in the temperature range between 473 and 573 K. It can be seen that oxygen was completely consumed at all studied temperatures. CH_3OH conversion, H_2 selectivity and CO selectivity were increased with temperature. It was proposed that when the temperature was increased, the contribution of MC, WGS, SRM and MD reactions were occurred [17,47]. Also, in the figure, CH_3OH conversion passes through two inflexion points. This suggests that different reaction mechanisms may occur during methanol partial oxidation. Initially, in the low temperature region (473–498 K), along with POM (Eq. (4)), methanol may quickly consumed oxygen leading to highly exothermic MC reaction to occur and produced H_2O and CO_2 (Eq. (6)) [19,49]. When temperature increased from 498 to 523 K, the involvement of MC was less compared to POM. More H_2 was produced by POM reaction. Further increase of temperature (523–573 K), along with POM the steam produced by MC was consumed by SRM reaction, which leads to increase H_2 selectivity [44]. At high temperature, MD reaction was predominated leading to more H_2 and CO formation. It was reported that MD reaction starts beyond 523 K [19]. Besides, the CO formed by MD and H_2O formed by MC react to pursue WGS reaction and forms CO_2 and H_2 (Eq. (5)). A little high CO selectivity (12%) at 573 K suggests that MD was faster than WGS at this temperature.

The activity and stability of copper supported on rice husk ash and commercial silica gel were compared for POM at 523 K. It can be seen from Fig. 10 that at the initial stage of reaction, Cu/SiO_2 catalyst showed little higher CH_3OH conversion and H_2 selectivity than Cu/RHA catalyst. However, the Cu/SiO_2 catalyst was deactivated with faster rate than Cu/RHA catalyst. It is important to note that the Cu/SiO_2 catalyst produced more CO, the undesirable by-product. Surface properties of these catalysts shows that the Cu/RHA catalyst exhibited highly dispersed small copper crystallites possessing higher copper surface area than Cu/SiO_2 catalyst (Table 1). It was reported that for POM using supported copper catalysts, metallic Cu is selective towards H_2 and CO_2 formation, while Cu^+ favors H_2O and CO formation and Cu^{2+} shows very low activity, which leads to CO_2 and H_2O [43]. The higher CO selectivity over Cu/SiO_2 catalyst might be due to lower copper surface area. The higher rate of deactivation of Cu/SiO_2 could be attributed to the catalyst surface possessing smaller pores, which might be feasibly clogged or sealed during sintering, resulted in the loss of copper surface area. Supporting evidence is from our previous studies [32,33], which have reported smaller pore size in Cu/SiO_2 catalyst than in Cu/RHA catalyst. The surface pores on RHA are unique pores, while those on SiO_2 are interconnected pores. The copper particles on SiO_2 may easily be blocked during thermal activation or catalytic reaction. It is important to note that compared to copper supported on other supports, the silica extracted from rice husk exhibited higher activity and selectivity. For instance, the Cu/Cr catalyst has exhibited 82.3% H_2 selectivity and 13.5% CO selectivity at 523 K [50]. The carbon nanotubes supported Cu–Zn catalyst has exhibited 70.6% H_2 selectivity and 8% CO at 533 K [51]. Although the reaction conditions used by Agrell et al. [49] have little difference from the present study, the Cu/ZnO catalyst showed low activity. The CH_3OH conversion was 15% and H_2 yield was 14% at 523 K. The presently studied catalyst, copper supported on RHA exhibited 87% CH_3OH conversion, 92.5% H_2 selectivity and 2.9% CO selectivity. Additional advantage of this catalyst is other by-products such as, formaldehyde, dimethyl ether, methyl formate or formic acid were not detected, which commonly observed in other copper supported catalysts. The Cu/Cr catalyst produced formaldehyde, methyl formate and dimethyl ether. The Cu/ZnO catalyst produced formaldehyde by-product. The present study demonstrates the use of copper supported on silica extracted from rice husk for selective hydrogen production by POM. As Cu/RHA catalyst proves to be an active catalyst for selective production of H_2, it finds application as a suitable catalyst for fuel cell application.

4. Conclusions

Rice husk ash was used as a support to copper for partial oxidation of methanol to produce hydrogen. The TPR studies show that increase in Cu loading increases the reduction temperature. The XPS results reveal that the catalyst precursor mainly exists as $Cu(OH)_2$. The catalyst under reduction treatment the CuO is reduced to Cu^0.

The catalytic activity at different calcination temperatures indicates that the catalytic activity decreases beyond 673 K. The catalytic activity at various reaction temperatures shows that the CH_3OH conversion, H_2 selectivity and CO selectivity increase with reaction temperature. Comparison of Cu/RHA and Cu/SiO_2 demonstrates that initially the Cu/SiO_2 catalyst has little higher CH_3OH conversion and H_2 selectivity than Cu/RHA catalyst. However, the activity of Cu/SiO_2 catalyst deactivates with faster rate than Cu/RHA catalyst.

Acknowledgements

The authors express thanks to the National Science Council of Taiwan for its financial support under project NSC 96-2221-E-008-055.

References

[1] J. St-Pierre, D.P. Wilkinson, AIChE J. 47 (2001) 1482–1486.
[2] A. Folkesson, C. Andersson, P. Alvfors, M. Alaküla, L. Overgaard, J. Power Sources 118 (2003) 349–357.
[3] J.J. Hwang, D.Y. Wang, N.C. Shih, D.Y. Lai, C.K. Chen, J. Power Sources 133 (2004) 223–228.
[4] J.J. Hwang, D.Y. Wang, N.C. Shih, J. Power Sources 141 (2005) 108–115.
[5] C. Wang, Z. Mao, F. Bao, X. Li, X. Xie, Int. J. Hydrogen Energy 30 (2005) 1031–1034.
[6] K. Tüber, M. Zobel, H. Schmidt, C. Hebling, J. Power Sources 122 (2003) 1–8.
[7] L.F. Brown, Int. J. Hydrogen Energy 26 (2001) 381–397.
[8] S.T. Yong, K. Hidajat, S. Kawi, Catal. Today 131 (2008) 188–196.
[9] P.H. Matter, U.S. Ozkan, J. Catal. 234 (2005) 463–475.
[10] S.S.Y. Lin, W.J. Thomson, T.J. Hagensen, S.Y. Ha, Appl. Catal. A 318 (2007) 121–127.
[11] M. Turco, G. Bagnasco, U. Costantino, F. Marmottini, T. Montanari, G. Ramis, G. Busca, J. Catal. 228 (2004) 56–65.
[12] M. Turco, G. Bagnasco, C. Cammarano, P. Senese, U. Costantino, M. Sisani, Appl. Catal. B 77 (2007) 46–57.
[13] A. Kulprathipanja, J.L. Falconer, Appl. Catal. A 261 (2004) 77–86.
[14] M.L. Cubeiro, J.L.G. Fierro, J. Catal. 179 (1998) 150–162.
[15] J. Divisek, H.F. Oetjen, V. Peinecke, V.M. Schmidt, U. Stimming, Electrochim. Acta 43 (1998) 3811–3815.
[16] J. Agrell, G. Germani, S.G. Järås, M. Boutonnet, Appl. Catal. A 242 (2003) 233–245.
[17] R. Ubago-Pérez, F. Carrasco-Marín, C. Moreno-Castilla, Catal. Today 123 (2007) 158–163.
[18] A. Wan, C.T. Yeh, Catal. Today 129 (2007) 293–296.
[19] F.-W. Chang, L.S. Roselin, T.-C. Ou, Appl. Catal. A 334 (2008) 147–155.
[20] F.-W. Chang, S.-C. Lai, L.S. Roselin, J. Mol. Catal. A: Chem. 282 (2008) 129–135.
[21] T.J. Huang, S.W. Wang, Appl. Catal. 24 (1986) 287–297.
[22] R.M. Navarro, M.A. Pena, C. Merino, J.L.G. Fierro, Top. Catal. 30/31 (2004) 481–486.
[23] F.-W. Chang, T.-J. Hsiao, J.-D. Shih, Ind. Eng. Chem. Res. 37 (1998) 3838–3845.
[24] F.-W. Chang, H.-C. Yang, L.S. Roselin, W.-Y. Kuo, Appl. Catal. A 304 (2006) 30–39.
[25] F. Adam, K. Kandasamy, S. Balakrishnan, J. Colloid Interface Sci. 304 (2006) 137–143.
[26] F. Adam, J. Andas, J. Colloid Interface Sci. 311 (2007) 135–143.
[27] A.E. Ahmed, F. Adam, Micropor. Mesopor. Mater. 103 (2007) 284–295.
[28] F. Adam, A.E. Ahmed, Chem. Eng. J. 145 (2008) 328–334.
[29] A.E. Ahmed, F. Adam, Micropor. Mesopor. Mater. 118 (2009) 35–43.
[30] F. Adam, P. Retnam, A. Iqbal, Appl. Catal. A 357 (2009) 93–99.
[31] F.-W. Chang, M.-T. Tsay, S.-P. Liang, Appl. Catal. A 209 (2001) 217–227.
[32] F.-W. Chang, W.-Y. Kuo, H.-C. Yang, Appl. Catal. A 288 (2005) 53–61.
[33] F.-W. Chang, W.-Y. Kuo, K.-C. Lee, Appl. Catal. A 246 (2003) 253–264.
[34] C.J.G. van der Grift, P.A. Elberse, A. Mulder, J.W. Geus, Appl. Catal. 59 (1990) 275–289.
[35] C.J.G. van der Grift, A.F.H. Wielers, B.P.J. Joghi, J. van Beijnum, M. de Boer, M. Versluijs-Helder, J.W. Geus, J. Catal. 131 (1991) 178–189.
[36] C.J.G. van der Grift, A.F.H. Wielers, A. Mulder, J.W. Geus, Thermochim. Acta 171 (1990) 95–113.
[37] E.D. Guerreiro, O.F. Gorriz, G. Larsen, L.A. Arrúa, Appl. Catal. A 204 (2000) 33–48.
[38] W. Baowei, Z. Xu, X. Qian, X. Genhui, Chin. J. Catal. 29 (2008) 275–280.
[39] N. Yalcin, V. Sevinc, Ceram. Int. 27 (2001) 219–224.
[40] A. Yin, X. Guo, W.-L. Dai, H. Li, K. Fan, Appl. Catal. A 349 (2008) 91–99.
[41] M.F. Luo, P. Fang, M. He, Y.L. Xie, J. Mol. Catal. A: Chem. 239 (2005) 243–248.
[42] C.J.G. van der Grift, A. Mulder, J.W. Geus, Appl. Catal. 60 (1990) 181–192.
[43] L. Alejo, R. Lago, M.A. Peña, J.L.G. Fierro, Appl. Catal. A 162 (1997) 281–297.
[44] J. Agrell, H. Birgersson, M. Boutonnet, I. Melián-Cabrera, R.M. Navarro, J.L.G. Fierro, J. Catal. 219 (2003) 389–403.
[45] Z. Wang, W. Wang, G. Lu, Int. J. Hydrogen Energy 28 (2003) 151–158.
[46] S. Velu, K. Suzuki, T. Osaki, Catal. Lett. 62 (1999) 159–167.
[47] J. Agrell, K. Hasselbo, K. Jansson, S.G. Järås, M. Boutonnet, Appl. Catal. A 211 (2001) 239–250.
[48] I.A. Fisher, A.T. Bell, J. Catal 184 (1999) 357–376.
[49] J. Agrell, M. Boutonnet, J.L.G. Fierro, Appl. Catal. A 253 (2003) 213–223.
[50] Z. Wang, J. Xi, W. Wang, G. Lu, J. Mol. Catal. A: Chem. 191 (2003) 123–134.
[51] I. Eswaramoorthi, V. Sundaramurthy, A.K. Dalai, Appl. Catal. A 313 (2006) 22–34.